Supporting information

Aggregation-induced emission and clusterization-triggered emission united in mesoporous silica nanoparticles for construction of efficient artificial light-harvesting system

Saisai Yan,[abc] Zhinong Gao,*[ac] Hongyan Yan,[d] Fei Niu[a] and Zhengqin Zhang[ac]

[a] Key Laboratory of Biomedical Polymers of Ministry of Education, College of Chemistry and Molecular Sciences, Wuhan University, Wuhan 430072, Hubei, P.R. China.

[b] College of Physics and Optoelectronic Engineering, Shenzhen University, Shenzhen 518060, China

[c] Engineering Research Center of Organosilicon Compounds & Materials of Ministry of Education, College of Chemistry and Molecular Sciences, Wuhan University, Wuhan 430072, Hubei, P.R. China.

[d] Shandong Institute for Product Quality Inspection, Jinan, 250102 Shandong, P. R. China

*Corresponding author: Zhinong Gao

E-mail: gzn@whu.edu.cn; whugzn@aliyun.com

Table of Contents

1. Supplementary Figures

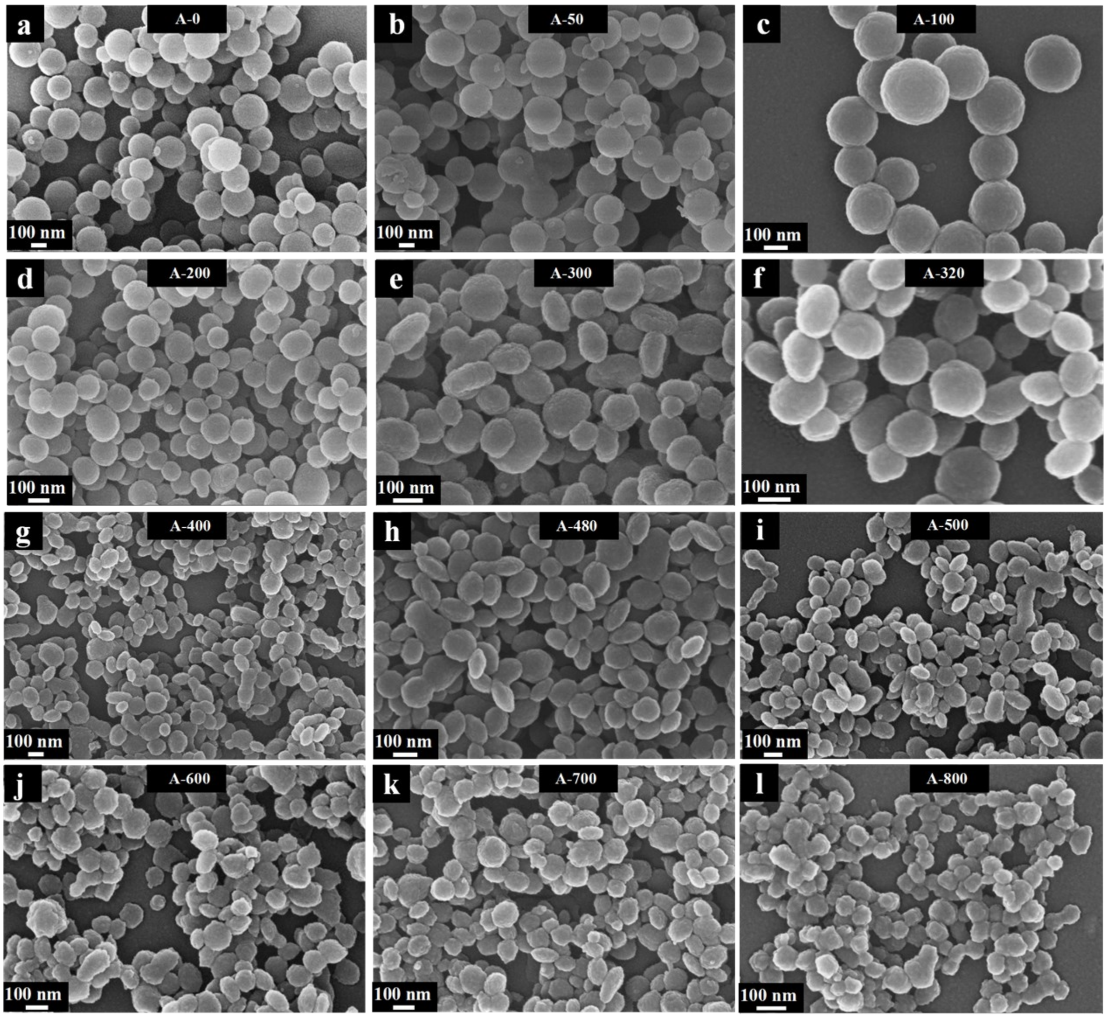

Figure S1. SEM images of SNs obtained under different concentrations of C_{TPE}-C_6-C_{TPE}: (a) 0, (b) 50, (c) 100, (d) 200, (e) 300, (f) 320, (g) 400, (h) 480, (i) 500, (j) 600, (k) 700, (l) 800 μM.

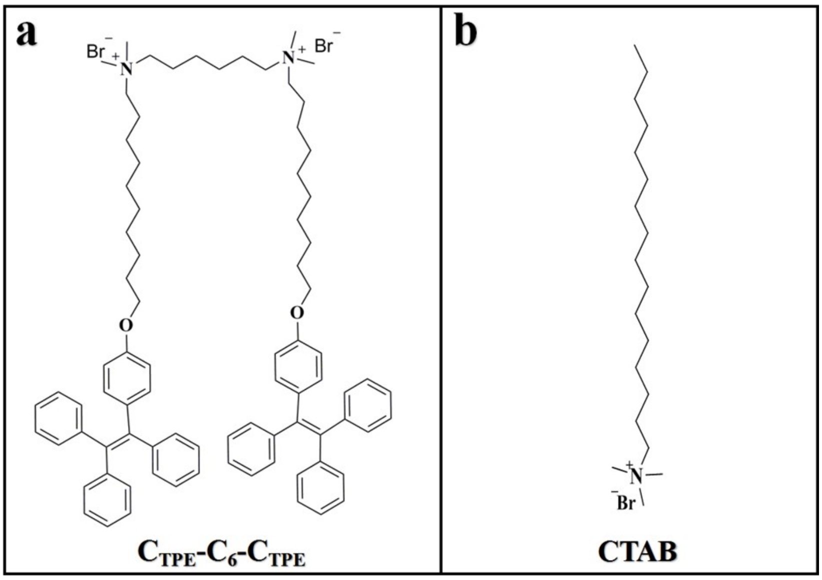

Figure S2. The chemical structures of C_{TPE}-C_6-C_{TPE} (a) and CTAB (b).

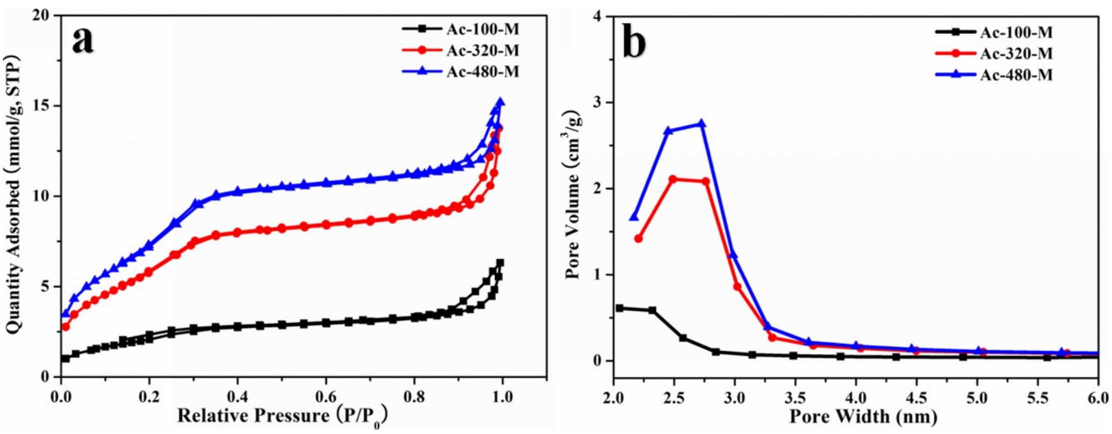

Figure S3. Nitrogen adsorption-desorption isotherms (a) and their corresponding pore size distribution curves (b) of Ac-100-M, Ac-320-M and Ac-480-M.

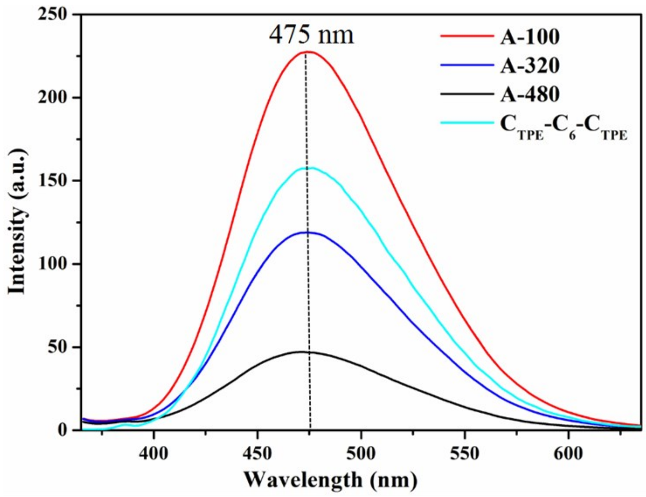

Figure S4. Fluorescence spectra of A-100, A-320, A-480 and C_{TPE}-C_6-C_{TPE}.

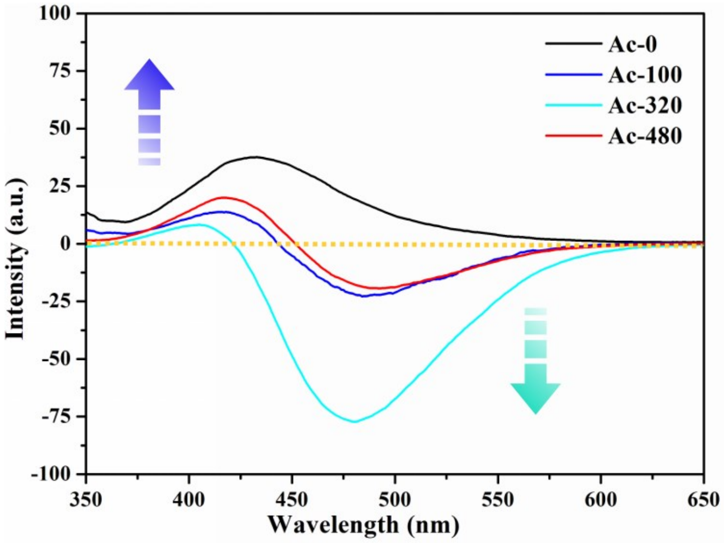

Figure S5. The difference in fluorescence intensity of Ac-0, Ac-100, Ac-320 and Ac-480 after being treated with ethanol.

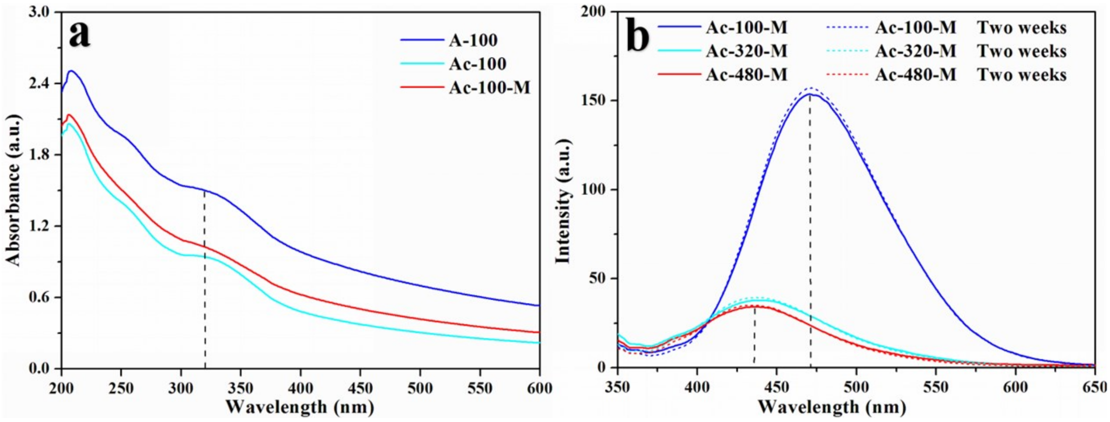

Figure S6. (a) Absorption spectra of A-100, Ac-100 and Ac-100-M aqueous dispersion in PBS (0.4 mg/mL). (b) Time-dependent evolution of the fluorescence intensity of Ac-100-M, Ac-320-M and Ac-480-M.

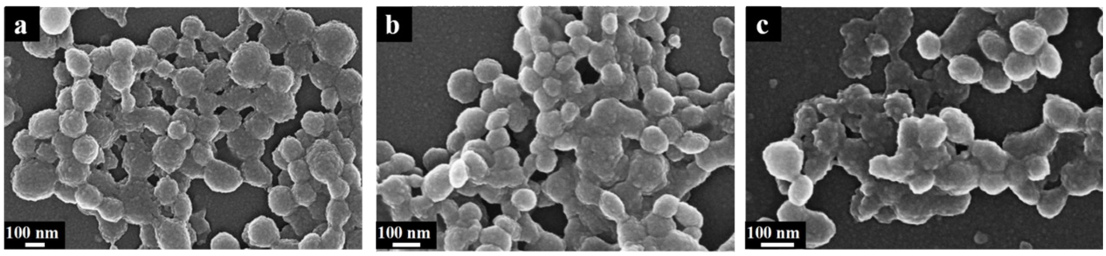

Figure S7. SEM images of Ac-100-M at pH=5.5 (a), Ac-320-M at pH=5.5 (b) and Ac-480-M at pH=4.8 (c) after two weeks.

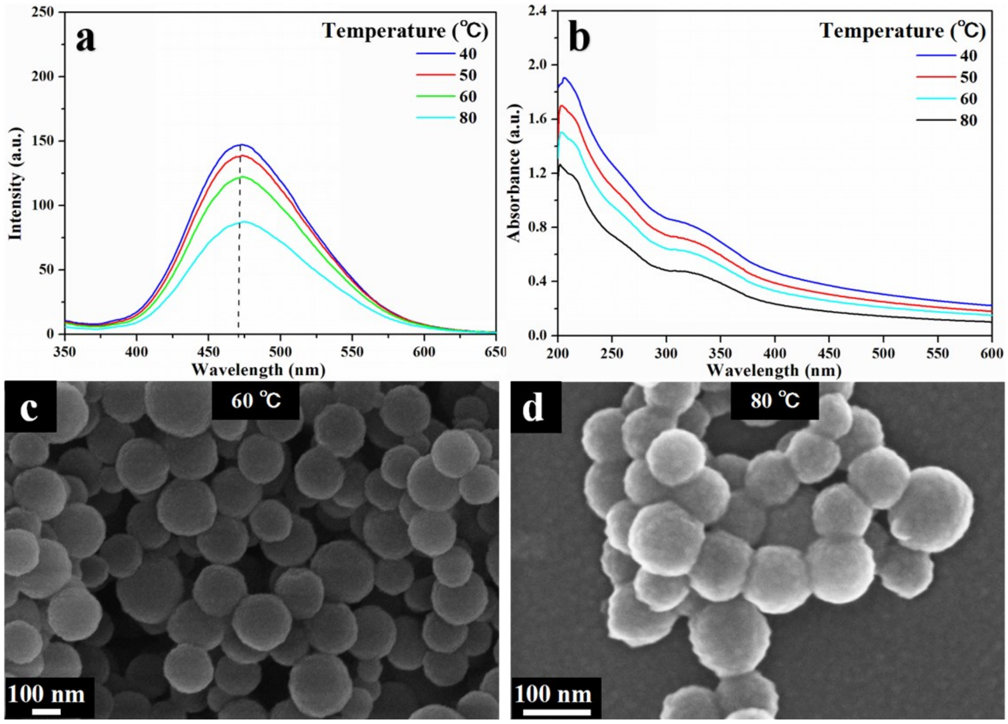

Figure S8. Fluorescence spectra (a) and absorption spectra (b) of Ac-100-M after treatment with different temperatures. SEM images of Ac-100-M after treatment with 60 ºC (c) and 80 ºC (d).

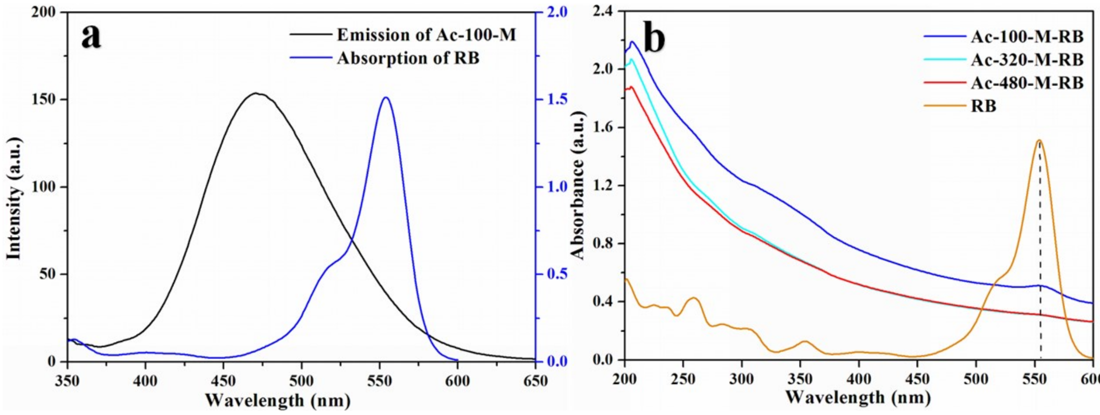

Figure S9. (a) Emission spectrum of Ac-100-M upon excitation at 340 nm and absorption spectrum of RB in PBS. (b) Absorption spectra of Ac-100-M-RB, Ac-320-M-RB, Ac-480-M-RB and RB. The immersion concentrations for MSNs were determined as 500 µM.

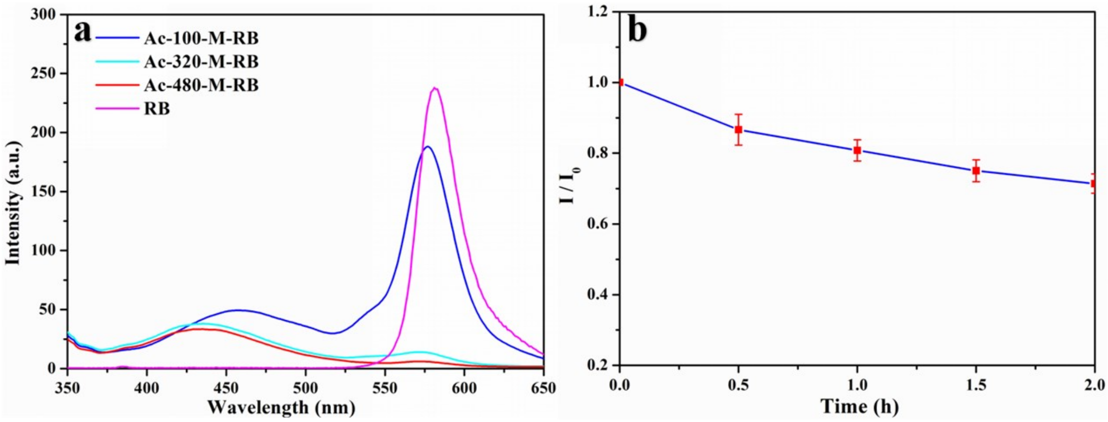

Figure S10. (a) Fluorescence spectra of Ac-100-M-RB, Ac-320-M-RB, Ac-480-M-RB and RB upon excitation at 340 nm. The immersion concentrations for MSNs were determined as 500 μM. (b) Photostability of Ac-100-M-RB upon continuous UV excitation. I_0 is the initial fluorescence intensity at 575 nm and I is the fluorescence intensity of the samples after UV irradiation.

2. Fluorescence lifetime measurements

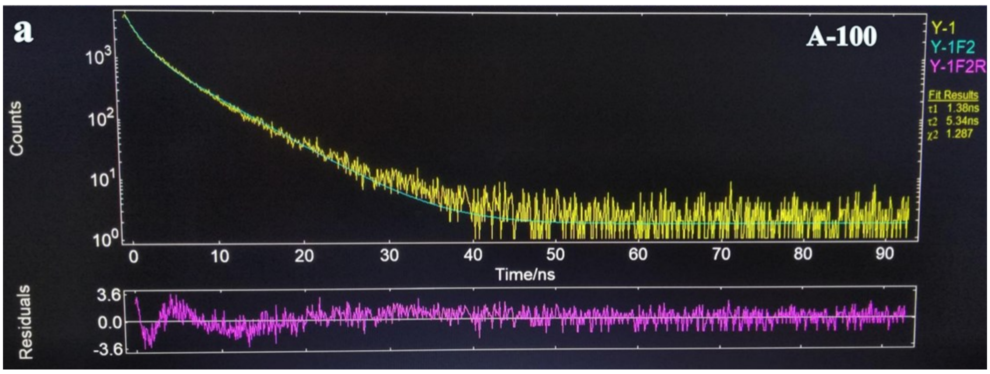

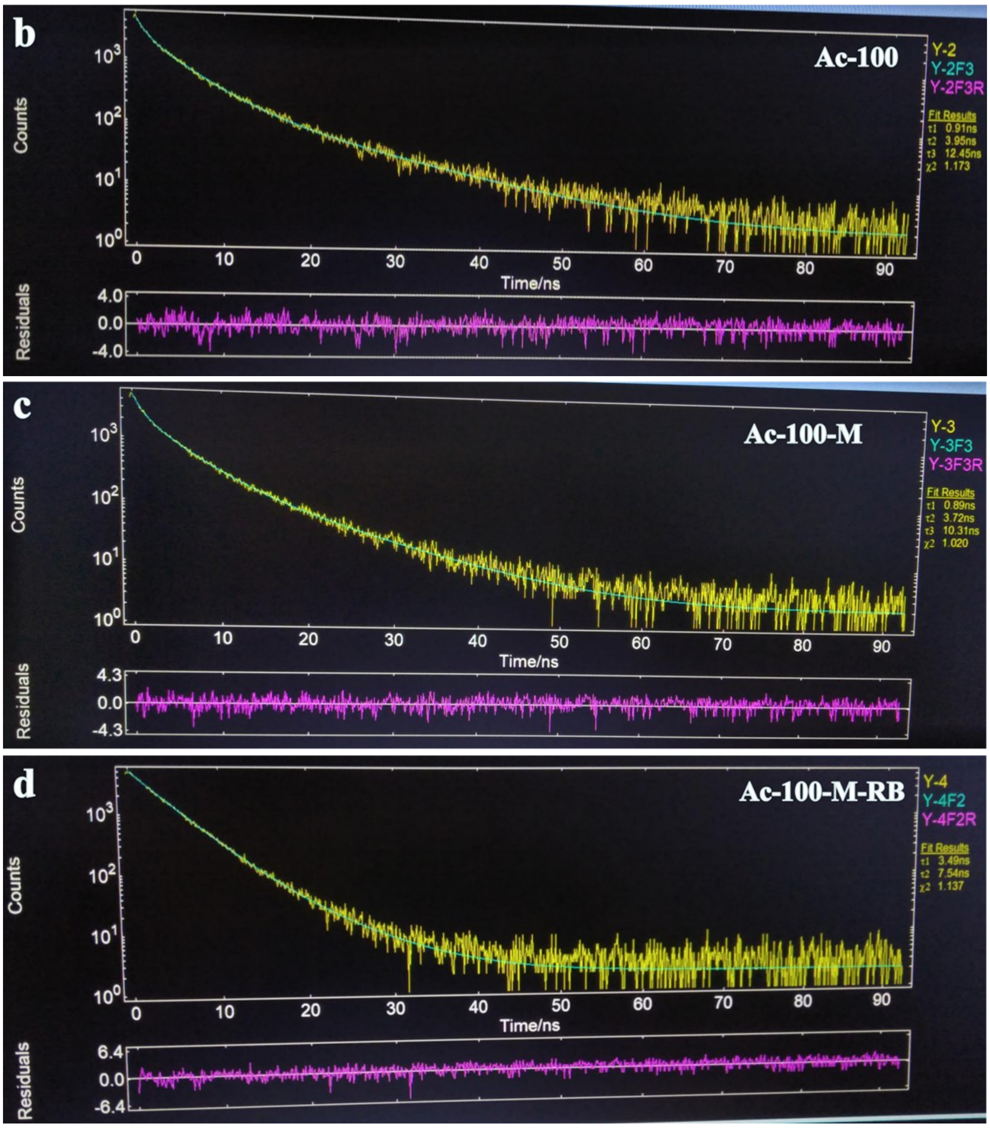

Figure S11. The fluorescence decay profiles of A-100 (a), Ac-100 (b), Ac-100-M (c) and Ac-100-M-RB (d).

3. Quantum yield measurements

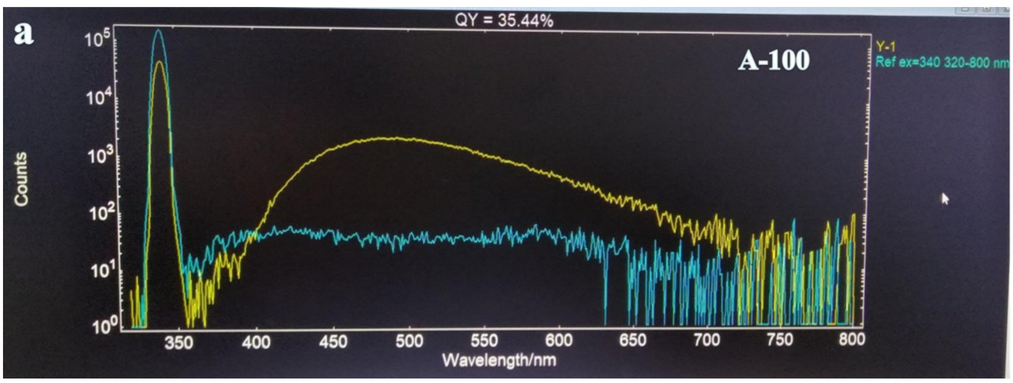

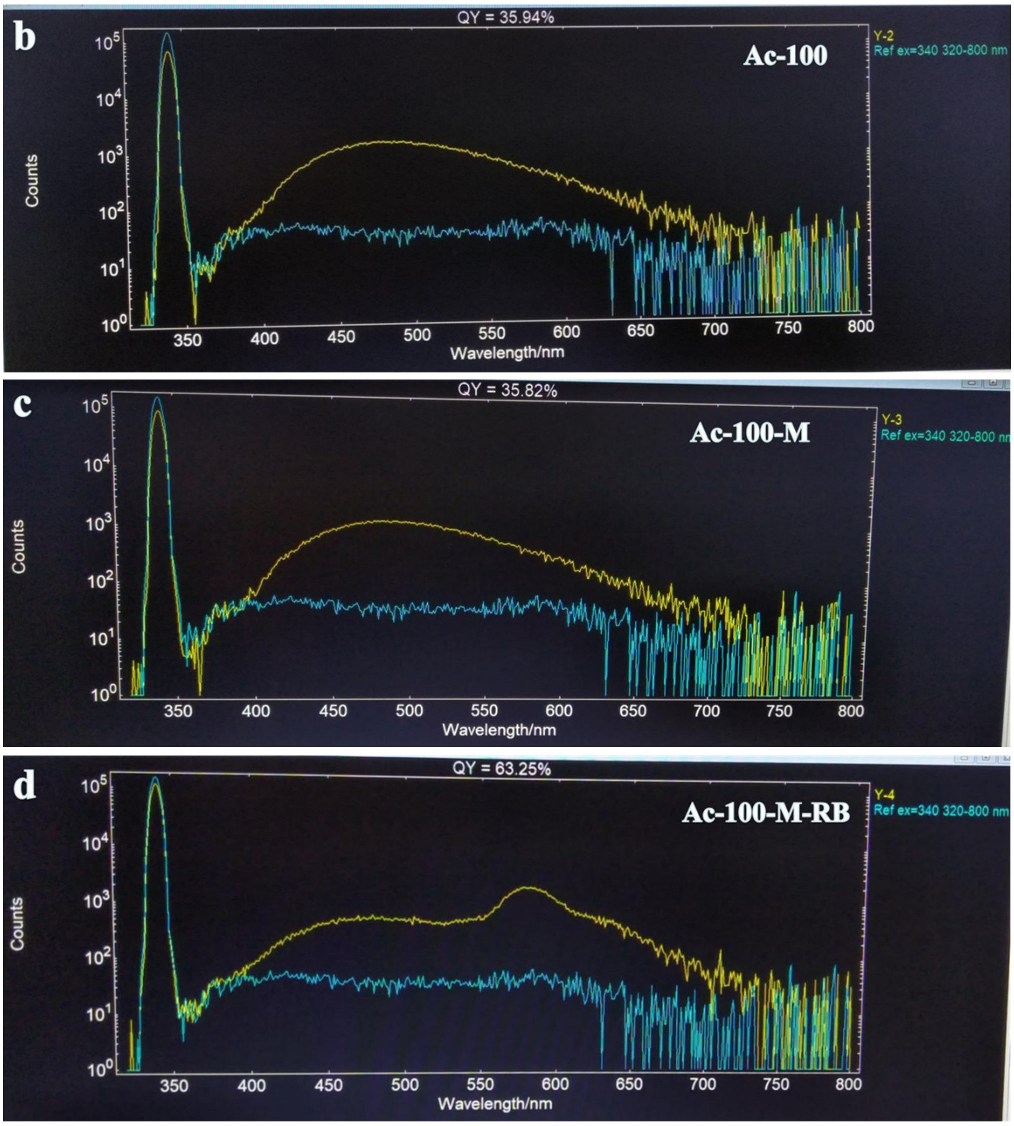

Figure S12. The absolute fluorescence quantum yields (QY) of A-100 (a), Ac-100 (b), Ac-100-M (c) and Ac-100-M-RB (d).

4. Calculation of energy-transfer efficiency (Φ)

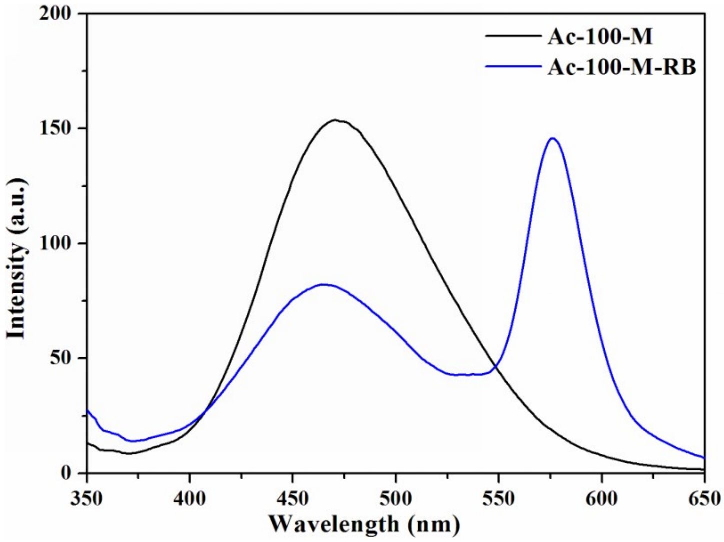

Figure S13. Fluorescence spectra of Ac-100-M and Ac-100-M-RB upon excitation at 340 nm.

Energy-transfer efficiency (Φ) was calculated from excitation fluorescence spectra through the equation: $\Phi = 1\text{-}I_{DA}/I_D$

Where I_{DA} and I_D are the fluorescence intensities of the emission of Ac-100-M-RB (donor and acceptor) and Ac-100-M (donor) respectively when excited at 340 nm (Figure S13).

The energy-transfer efficiency was calculated as 46.9% in aqueous environment, the measuring Ac-100-M-RB was prepared under the condition of RB=70 μM.

5. Calculation of antenna effect (*AE*)

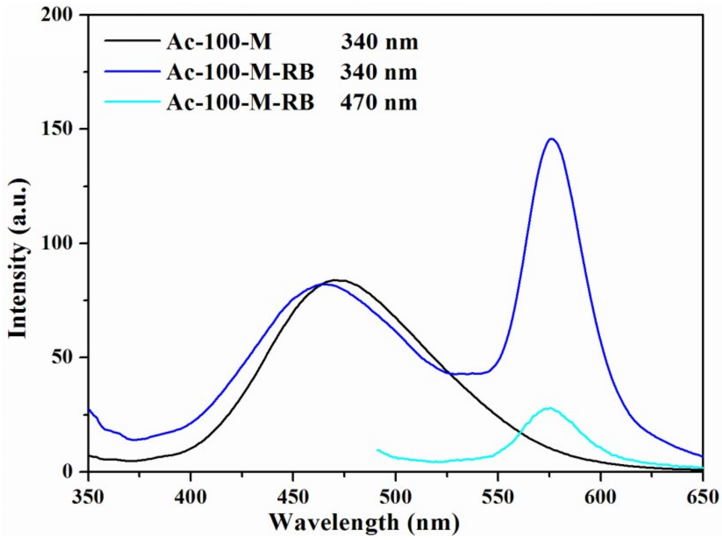

Figure S14. Fluorescence spectra of the Ac-100-M-RB aqueous dispersion (blue line), cyan line (acceptor emission, λ_{ex}=470 nm). The black line represents the fluorescence spectrum of Ac-100-M, which was normalized according to the fluorescence intensity at 470 nm of the blue line.

The energy-transfer efficiency (Φ) was calculated as 46.9% in aqueous environment, the measuring Ac-100-M-RB prepared under the condition of RB=70 μM.

The antenna effect (*AE*) was calculated based on the excitation spectra using equation: $AE = (I_{DA,340} - I_{D,340})/I_{DA,\ 470}$

Where $I_{DA,340}$ and $I_{DA,\ 470}$ are the fluorescence intensities at 575 nm with the excitation of the donor at 340 nm and the direct excitation of the acceptor at 470 nm, respectively. $I_{D,340}$ is the fluorescence intensities at 575 nm of Ac-100-M, which was normalized with the Ac-100-M-RB at 470 nm (Figure S14).

The antenna effect value was calculated as 4.9 in aqueous environment, the measuring Ac-100-M-RB was prepared under the condition of RB=70 μM

6. Supplementary Tables

Table S1. A summary of experimental data and processing parameters.

Samples	Volume ratio of TEOS/APS	C^a (μM)	Morphology
A-0	1:1	0	Coarse nanospheres
A-50	1:1	50	Irregular nanospheres
A-100	1:1	**100**	Nanospheres
A-200	1:1	200	Rough nanospheres
A-300	1:1	300	Irregular pie-like nanoparticles
A-320	1:1	**320**	Pie-like nanoparticles
A-400	1:1	400	Irregular pie-like nanoparticles
A-480	1:1	**480**	Dish-like nanoparticles
A-500	1:1	500	Irregular dish-likenanoparticles
A-600	1:1	600	Irregular nanoparticles
A-700	1:1	700	Irregular nanoparticles
A-800	1:1	800	Irregular coarse nanoparticles

[a] The initial concentration of C_{TPE}-C_6-C_{TPE} in the reaction system.

Table S2. The structural properties of as-prepared Ac-100-M, Ac-320-M and Ac-480-M.

Samples	BET surface area (m^2/g)	Pore volume (cm^3/g)	Pore size (nm)
Ac-100-M	194.81	0.223	9.9
Ac-320-M	485.25	0.541	4.0
Ac-480-M	602.15	0.604	3.5

Table S3. The elemental content of as-prepared Ac-0-M, Ac-100-M, Ac-320-M and Ac-480-M by elemental analysis.

Samples	Elemental content (wt. %)		
	C	H	**N**
Ac-0-M	15.02	3.841	**3.821**
Ac-100-M	16.03	4.059	**4.070**
Ac-320-M	16.02	3.975	**4.010**
Ac-480-M	16.26	4.005	**3.902**

Table S4. The zeta-potential (ζ-potential) of as-prepared Ac-0-M, Ac-100-M, Ac-320-M and Ac-480-M.

Samples	ζ (mv)
Ac-0-M	20.4
Ac-100-M	22.8
Ac-320-M	28.6
Ac-480-M	26.8

Table S5. Fluorescence lifetimes of A-100 (monitored at 475 nm), Ac-100 (monitored at 470 nm), Ac-100-M (monitored at 470 nm) and Ac-100-M-RB (monitored at 575 nm).

Samples	τ_1 (ns)	RW_1 (%)	τ_2 (ns)	RW_2 (%)	τ_3 (ns)	RW_3 (%)	τ_{ave} (ns)	χ^2
A-100	1.3817	36.17	5.3449	63.83	/	/	**3.91**	1.287
Ac-100	0.9059	12.45	3.9482	62.35	12.4548	25.19	**5.71**	1.173
Ac-100-M	0.8894	15.14	3.7226	57.86	10.3105	27.01	**5.07**	1.020
Ac-100-M-RB	3.4851	87.56	7.5413	12.44	/	/	**3.99**	1.137

Table S6. The absolute fluorescence quantum yields of A-100, Ac-100, Ac-100-M, Ac-100-M and Ac-100-M-RB in PBS dispersion.

Samples	Fluorescence Quantum Yield ($\Phi_{f(abs)}$, %)
A-100	35.44
Ac-100	35.94
Ac-100-M	35.82
Ac-100-M-RB	63.25

Table S7. Comparison of the absolute fluorescence quantum yield ($\Phi_{f(abs)}$) of white light-emitting systems in various ALHSs.

Samples	Construction	$\Phi_{f(abs)}$ (%)	Ref.
AIE@cRVs	Cross-linked reverse vesicle with AIE-based fluorophores	38.0	1
CPSN	Conjugated polymeric supramolecular network	23.8	2
WP5/BPT-DBT-NiR	Supramolecular Pillar[5]arene polymers with enhanced AIE effect	23.5	3
GC4A/TP-TPE/DBT	Macrocyclic amphiphile calixarene with AIE-based fluorophores	19.0	4
AmC5A/1,8-ANS /DBT	Macrocyclic amphiphile calixarene	10.2	5
WP5/TPEDA-ESY - NiR	Supramolecular Pillar[5]arene polymers with AIE effect	5.01	6
Ac-100-M-RB	Fluorescent MSNs with AIE and CTE effect	**63.25**	This work

7. References

1. C. Li, J. Zhang, S. Zhang and Y. Zhao, *Angew. Chem. Int. Ed.*, 2019, **58**, 1643-1647.
2. L. Xu, Z. Wang, R. Wang, L. Wang, X. He, H. Jiang, H. Tang, D. Cao and B. Z. Tang, *Angew. Chem. Int. Ed.*, 2020, **59**, 9908-9913.
3. G. Sun, W. Qian, J. Jiao, T. Han, Y. Shi, X. Hu and L. Wang, *J. Mater. Chem. A*, 2020, **8**, 9590-9596.
4. W. Geng, Y. Liu, Y. Wang, Z. Xu, Z. Zheng, C. Yang and D. Guo, *Chem. Commun.*, 2017, **53**, 392-395.
5. Z. Xu, S. Peng, Y. Wang, J. Zhang, A. I. Lazar and D. Guo, *Adv. Mater.*, 2016, **28**, 7666-7671.
6. M. Hao, G. Sun, M. Zuo, Z. Xu, Y. Chen, X.-Y. Hu and L. Wang, *Angew. Chem. Int. Ed.*, 2020, **59**, 10095-10100.